



## A New Polymeric Nanocomposite Coating for Corrosion Protection of Carbon Steel in HCl Solution

M. Shahidi\*, Gh. Golestani

Department of Chemistry, Kerman Branch, Islamic Azad University, P.O. Box: 76169-14111, Kerman, Iran.

### ARTICLE INFO

#### Article history:

Received: 02 May 2017

Final Revised: 09 Dec 2017

Accepted: 10 Dec 2017

Available online: 25 Dec 2017

#### Keywords:

YAG Nanoparticles

Polyvinyl Butyral

Protection Efficiency

Electrochemical Impedance Spectroscopy (EIS).

### ABSTRACT

*In the present work, four polymeric nanocomposite (PNC) coatings were prepared with different concentrations of yttrium aluminum garnet nanoparticles (YAG-NPs) in polyvinyl butyral (PVB) matrix. The corrosion protection of the PNC coatings applied on the carbon steel surface was investigated in 1.0 M HCl solution by electrochemical impedance spectroscopy (EIS). The YAG-NPs were synthesized by pulse electrochemical method. The formation of YAG-NPs was confirmed by XRD and SEM analysis. The EIS data obtained from the coated samples both without and with YAG-NPs samples were fitted with an equivalent circuit containing two time constants. The protection efficiency values of the PNC coatings were calculated from EIS data. The PNC coating containing 0.025 wt% YAG-NPs as the efficient coating showed the best corrosion protection in HCl solution for immersion times up to 28 days. Prog. Color Colorants Coat. 11 (2018), 1-8 © Institute for Color Science and Technology.*

### 1. Introduction

The coatings are one of the most effective routes to establish the long-term corrosion protection of metallic materials[1]. Organic coatings are widely used to protect metals and alloys from corrosion [2-5]. The corrosion protection of metallic surfaces by the organic coatings is supplied using three options: inhibitive pigments, sacrificial fillers and barrier coatings [6]. Inhibitive pigments such as chromates are commonly applied on Alalloys while sacrificial coatings like zinc-rich primers provide the cathodic protection on the steel alloys. The protection caused by barrier coatings is probably due to their high electrical resistance. This prevents the external flow of ionic currents between anodic and cathodic areas.

The barrier effect can be improved by using appropriate fillers in the coating. The coatings loaded with nano-size fillers exhibit much higher barrier properties than those containing micron size additives [7, 8]. Therefore, the preparation and investigation of polymeric nanocomposite (PNC) coatings have provided a promising research field for corrosion protection [4, 6, 9, 10]. When nanoparticles are added to a coating, the micropores of the coating are filled by them and thereby, the diffusion is slowed down. For the coating without filler, only uniform diffusion can occur through intermolecular pores as shown in Figure 1(a) by dashed arrows. In the coating containing nanoparticle filler, the nanoparticles prevent uniform diffusion and introduce the mechanism of non-uniform diffusion (Figure 1(b)) [10].

\*Corresponding author: [shahidi@iauk.ac.ir](mailto:shahidi@iauk.ac.ir)

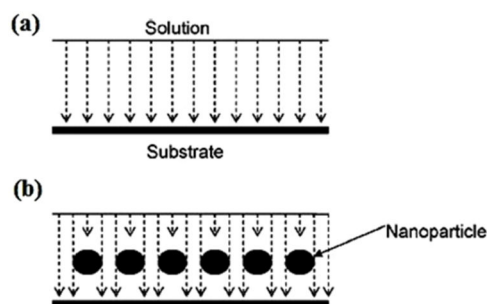


**Figure 1:** Schematic representation of diffusion into the coating: (a) coating without filler; (b) coating with nanoparticle filler [10].

Recently, a novel pulse electrochemical method was carried out for the synthesis of yttrium aluminum garnet (YAG:  $\text{Al}_5\text{Y}_3\text{O}_{12}$ ) nanoparticles in a mixture of  $\text{YCl}_3$  and  $\text{AlCl}_3$  aqueous solution [11]. In the present work, after preparation of the YAG nanoparticles (YAG-NPs) via the mentioned pulse method, the PNC coatings were prepared from polyvinyl butyral (PVB) matrix filled with various concentrations of YAG-NPs. Finally, the electrochemical impedance spectroscopy (EIS) was employed to evaluate the effect of PNC coatings on the corrosion protection of carbon steel in 1.0 M HCl solution.

## 2. Experimental

Polyvinyl butyral (PVB) of 40,000-70,000 MW was purchased from Acros Organics. All other chemical materials were purchased from Merck and used as received.

### 2.1. Preparation of YAG nanoparticles

This section briefly describes the preparation of YAG-NPs by pulse electrochemical synthesis at room temperature as previously reported [11]. The experiments were carried out in the three-electrode cell comprising 316L stainless steel as the working electrode, graphite as the counter electrode and saturated calomel electrode (SCE) as the reference electrode. The three electrodes were immersed in the solution of 0.005 M  $\text{YCl}_3 \cdot 6\text{H}_2\text{O}$ , 0.008 M  $\text{AlCl}_3 \cdot 6\text{H}_2\text{O}$  with pH adjusted to 2.7. By applying a peak current density of  $5 \text{ mA} \cdot \text{cm}^{-2}$  and  $t_{\text{on}} = t_{\text{off}} = 1 \text{ ms}$  for 20 min to the working electrode at  $60^\circ\text{C}$ , the thin films of YAG

were deposited on the surface of the steel. The square wave potential ( $-0.7 \text{ V}$  respect to SCE) was applied. After washing and drying of steel electrode, the deposited powders were scrapped. The heat-treatment of the powders was carried out in an electrical furnace at  $1200^\circ\text{C}$  for 2 h with the heating rate of  $5^\circ\text{C} \cdot \text{min}^{-1}$ . Transparent powders of YAG-NPs were finally formed. The formation of YAG nanoparticles was confirmed by the X-ray diffraction (XRD) and SEM as shown in Figures 2 and 3, respectively.

### 2.2. Preparation of coated samples

2 g of PVB was dissolved in 20 mL methanol with continuous stirring to prepare the PVB solution. The YAG-NPs powder was dispersed into the PVB solution with continuous stirring for 24 h to prepare the YAG-PVB dispersion. The YAG-NPs content in the coatings was 0, 0.0125, 0.025 and 0.05 wt%. These coated samples were symbolized as C0, C1, C2 and C5, respectively.

The coatings were applied on the surface of working electrodes made of carbon steel with the chemical composition (wt %) of: C (0.15), Mn (0.73), Si (0.72) and Fe (balance). Before coating application, the surface of working electrodes was abraded by wet abrasive papers through 600–2500 grade, washed with distilled water and degreased with ethanol. After drying in air, the working electrodes were dipped in the YAG-PVB dispersion for 30 s and baked in an air-circulating oven at  $50^\circ\text{C}$  for 12 h. Finally, the coated samples were immersed in a 1.0 M aqueous HCl solution.

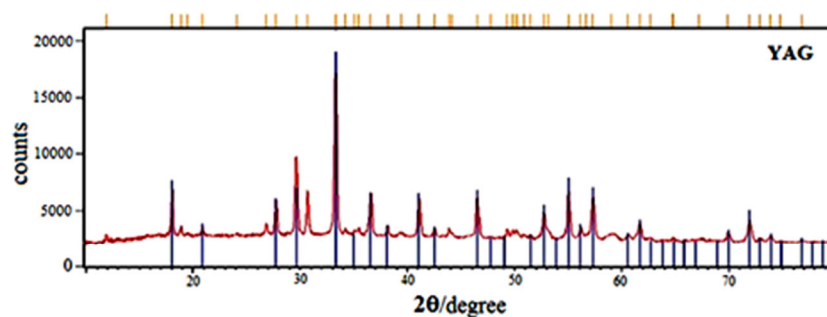


Figure 2: XRD spectrum of YAG.

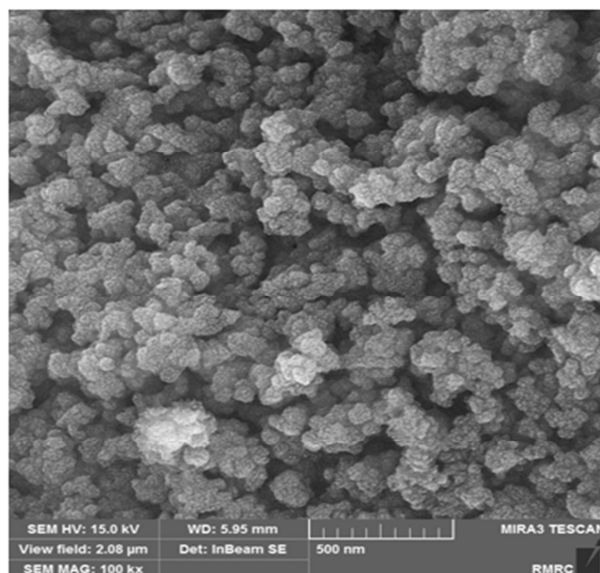


Figure 3: SEM image of YAG-NPs.

### 2.3. Corrosion tests

The EIS measurements were performed by applying a sinusoidal potential signal of 10 mV amplitude at OCP in the frequency range of 100 kHz-10 mHz. The EIS data were measured in a conventional three-electrode cell by a potentiostat/galvanostat (Autolab Model PGSTAT-302N). A platinum rod was used as the counter electrode, a saturated (KCl) Ag/AgCl electrode as the reference electrode and the coated carbon steel as the working electrode. The impedance data were analyzed with Nova 1.9 software.

### 3. Results and Discussion

The Bode plots of the coatings without (blank coating) and with different concentrations of YAG-NPs (PNC coatings) were obtained after immersing of the coated samples in 1.0 M HCl solution. Figure 4 shows the obtained plots at various times from 1 day to 28 days after immersion.

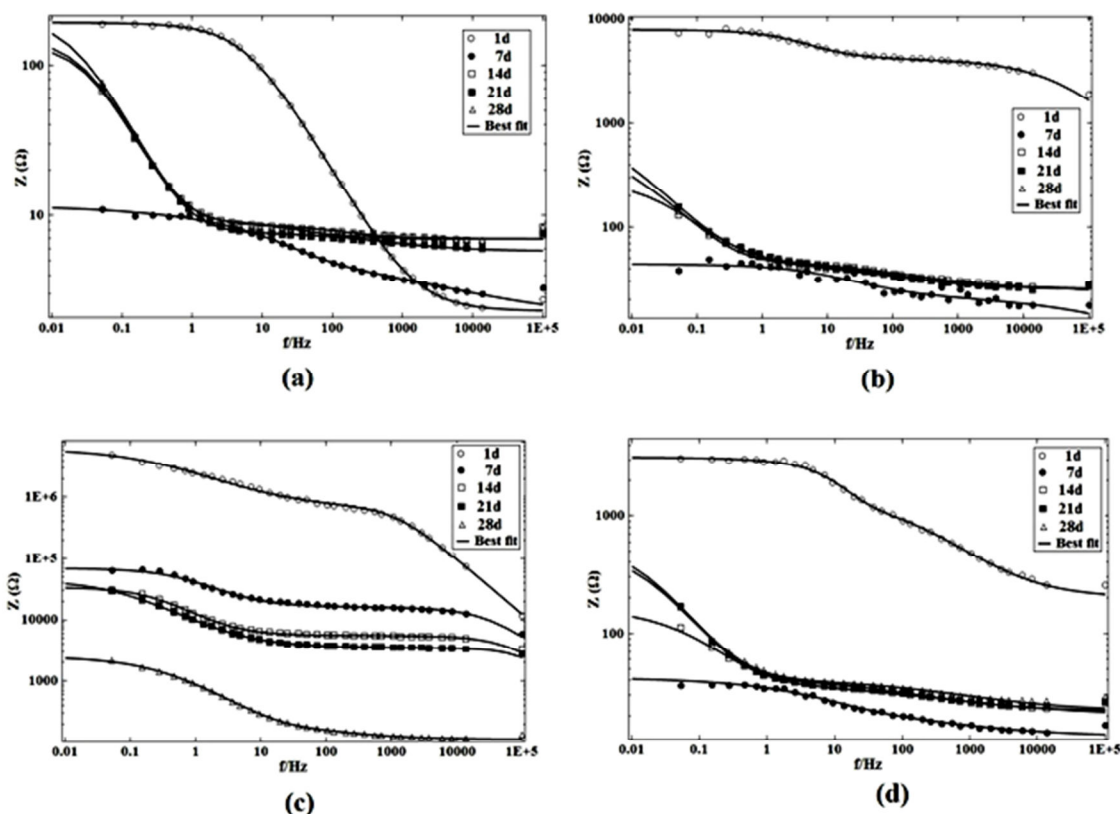


**Figure 4:** Bode plots of the coated samples with different concentrations of YAG-NPs at various times after immersion; (a) C0 (blank), (b) C1, (c) C2 and (d) C5.

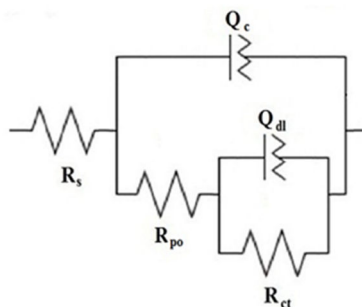


**Figure 5:** The equivalent circuit.

An equivalent circuit should be proposed to perform a detailed interpretation of the EIS data. The equivalent circuit shown in Figure 5 was selected for simulating the response of the studied system. The equivalent circuit consists of three resistances ( $R_s$ ,  $R_{po}$  and  $R_{ct}$ ) and two constant phase elements (CPE).  $R_s$  is the resistance of solution,  $R_{po}$  is the pore resistance and  $R_{ct}$  is the charge transfer resistance. Each of the two resistances of  $R_{po}$  and  $R_{ct}$  is associated with a corresponding CPE, representing the coating capacitance ( $Q_c$ ) and the double layer capacitance ( $Q_{dl}$ ).

$R_{po}$  is related to the permeability of the coating. The

charge transfer resistance,  $R_{ct}$ , as a measure of the kinetics of the corrosion process is proportionally inversed to the corrosion rate of the metallic surface.

The experimental EIS data were fitted to the equivalent circuit shown in Figure 5. The points in Figure 4 represent the experimental data, while the continuous lines represent the best fits. It can be observed that the fitted data match the experimental data. Table 1 lists the impedance parameters of the coated samples in the absence and presence of different concentrations of YAG-NPs at various times after immersion up to 28 days.

**Table 1:** The EIS parameters of various PVB coated samples in the absence and presence of different concentrations of YAG-NPs and the corresponding protection efficiency values.

$t_{\text{imm}}/\text{day}$	Sample	$R_{po}/k\Omega.cm^2$	$R_{ct}/k\Omega.cm^2$	PE (%)
1	C0	0.002	0.19	-
	C1	4.2	3.8	95
	C2	700	5740	99.99
	C5	1.24	1.74	89.1
7	C0	0.004	0.006	-
	C1	0.02	0.023	73.9
	C2	16.3	54	99.99
	C5	0.012	0.017	64.7
14	C0	0.002	0.12	-
	C1	0.025	0.255	52.9
	C2	5.6	29	99.6
	C5	0.019	0.145	17.2
21	C0	0.002	0.153	-
	C1	0.02	0.85	82
	C2	3.6	42	99.6
	C5	0.019	0.52	70.6
28	C0	0.003	0.18	-
	C1	0.03	1.45	87.6
	C2	0.129	2.32	92.2
	C5	0.019	0.6	70

Figure 6(a) depicts the corrosion resistance ( $R_{ct}$ ) values extracted from the EIS data of the blank coated sample, C0, given in Table 1. The blank coated sample suffered an important drop in corrosion resistance within the seven days of immersion, due to significant solution uptake through pores and thereby the corrosion of steel surface. After 7<sup>th</sup> day, the corrosion resistance increased rapidly with time up to 14<sup>th</sup> day of immersion and afterward it remained almost constant. This may be ascribed to the start of precipitation of corrosion products over the steel surface after 7 days of immersion.

The effect of different concentrations of YAG-NPs on the corrosion behavior of PNC coated samples in HCl solution can be evaluated using protection efficiency (PE) values, which are calculated by the following equation [12]:

$$PE = \frac{R'_{ct} - R_{ct}}{R'_{ct}} \times 100 \quad (1)$$

where  $R'_{ct}$  and  $R_{ct}$  are the charge transfer resistances of the coated samples with and without YAG-NPs, respectively. Table 1 presents the calculated PE values for the PNC coated samples (C1, C2 and C5). The charge transfer resistances,  $R_{ct}$ , for each set of four coated samples (C0, C1, C2 and C5) at a certain time of immersion were used for calculating the PE values of the PNC coatings at that time.

According to the PE values in Table 1, it can be deduced that C2 sample provided the highest corrosion protection at any time of immersion up to 28 days. The detailed evaluation of PNC coatings containing different concentrations of YAG-NPs can be achieved by the plot of PE vs. time using the data given in Table 1. Figure 6(b) demonstrates the evolution of protection efficiency for three PNC coatings (i.e. C1, C2 and C5) during immersion in 1.0 M HCl solution up to 28 days. Before the 14<sup>th</sup> day of immersion, the PE values decreased with time for both C1 and C5 coated samples.

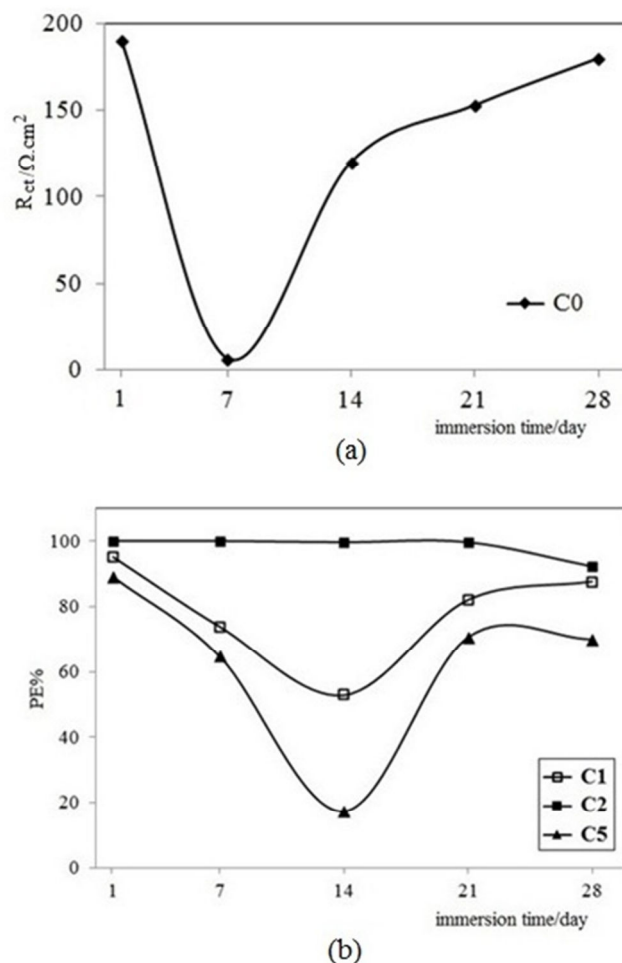


**Figure 6:** (a) The evolution of corrosion resistance,  $R_{ct}$ , for the blank coating, C0, and (b) the evolution of protection efficiency (PE) for three PNC coatings (C1, C2 and C5) during immersion in 1.0 M HCl solution.

This is due to the uptake of electrolyte through pores of coatings and thereby the corrosion of alloy surface. After 14 days of immersion, the precipitation of corrosion products led to the formation of a protective layer, which thickened with time up to 21 days and progressively hindered the corrosion processes. Therefore, from the 14<sup>th</sup> day of immersion, the protection efficiency increased with time up to the 21<sup>st</sup> day for both C1 and C5 samples and afterward it became almost constant up to the 28<sup>th</sup> day (Figure 6b).

It can be seen from Figure 6(b) that C2 coated sample showed the best corrosion protection for long immersion times up to 28 days. Therefore, it can be concluded that C2 sample is the efficient coating

containing the optimum concentration of YAG-NPs filler.

It is important to note that increase of nanoparticles concentration in the coated samples leads to both the decrease of the uniform diffusion (Figure 1) and the increase of the roughness of coating surface. The efficient coating is achieved under the optimum concentration of nanoparticles so that both the uniform diffusion and the surface roughness are minimized.

According to Figure 6(b), both C1 and C5 coated samples presented the low corrosion protection in comparison with the C2 sample. The lower corrosion protection of the C1 and the C5 samples can be attributed to the more uniform diffusion and the more

roughness of the coating surface, respectively. The more uniform diffusion in the C1 sample arises from the lower concentration of the YAG nanoparticles compared to the C2 sample. On the other hand, the more roughness of the C5 surface emanates from the higher concentration of the nanoparticles.

Coating capacitance is an important factor which is widely used for evaluating the protective performance of organic coatings. As it can be seen from Table 1, coating capacitance increased due to water penetration into the coating. The dielectric constant of water is larger than that of polymeric coatings. Consequently, water uptake within the coating increases the coating capacitance. According to Table 1, it was observed that the C2 sample has the lowest coating capacitance at any time after immersion.

Water uptake percentage of coatings ( $\Phi_w$  %) can be obtained according to Brasher-Kingsburg's equation (2) [12]:

$$\Phi_w \% = \frac{[\log(C_t/C_0)]}{\log(\epsilon_w)} \times 100 \quad (2)$$

## 5. References

1. M. Plawecka, D. Snihirova, B. Martins, K. Szczepanowicz, P. Warszynski, M.F. Montemor, Self healing ability of inhibitor-containing nanocapsules loaded in epoxy coatings applied on aluminium 5083 and galvaneal substrates, *Electrochim. Acta*, 140(2014) 282-293.
2. M.R. Mahmoudian, Y. Alias, W.J. Basirun, M. Ebadi, Effects of different polypyrrole/TiO<sub>2</sub> nanocomposite morphologies in polyvinyl butyral coatings for preventing the corrosion of mild steel, *Appl. Surf. Sci.*, 268(2013) 302-311.
3. M. Hasanzadeh, M. Shahidi, M. Kazemipour, Application of EIS and EN techniques to investigate the self-healing ability of coatings based on microcapsules filled with linseed oil and CeO<sub>2</sub> nanoparticles, *Prog. Org. Coat.*, 80 (2015) 106-119.
4. A. Ghasemi-Kahrizsangi, H. Shariatpanahi, J. Neshati, E. Akbarinezhad, Corrosion behavior of modified nano carbon black/epoxy coating in accelerated conditions, *Appl. Surf. Sci.*, 331(2015) 115-126.
5. A. Foyet, T.H. Wu, A. Kodentsov, L.G.J.v.d. Ven, G.d. With, R.A.T.M.v. Benthem, Corrosion Protection and Delamination Mechanism of Epoxy/Carbon Black Nanocomposite Coating on AA2024-T3, *J. Electrochem. Soc.*, 160(2013) C159-C167.
6. S. Radhakrishnan, C.R. Siju, D. Mahanta, S. Patil, G. Madras, Conducting polyaniline-nano-TiO<sub>2</sub> composites for smart corrosion resistant coatings, *Electrochim. Acta*, 54(2009) 1249-1254.
7. M. Tamilselvi, P. Kamaraj, M. Arthanareeswari, S. Devikala, Nano zinc phosphate coatings for enhanced corrosion resistance of mild steel, *Appl. Surf. Sci.*, 327(2015) 218-225.
8. V.V. Maslov, V.P. Yurinskii, N.A. Egorov, Adhesion and barrier properties of polymeric nanocomposite films, *Russ. J. Appl. Chem.*, 87(2014) 1700-1706.
9. D.E. Tallman, K.L. Levine, C. Siripiom, V.G. Gelling, G.P. Bierwagen, S.G. Croll, Nanocomposite of polypyrrole and alumina nanoparticles as a coating filler for the corrosion protection of aluminium alloy 2024-T3, *Appl. Surf. Sci.*, 254(2008) 5452-5459.
10. H. Mohammad Shiri, A. Ehsani, J. Shabani Shayeh, Synthesis and highly efficient supercapacitor behavior of a novel poly pyrrole/ceramic oxide nanocomposite film, *RSC Advances*, 5(2015) 91062-91068.

where  $C_t$  is the coating capacitance at time  $t$ ,  $C_0$  is the initial coating capacitance (one day after immersion) and  $\epsilon_w$  is the dielectric constant of water (80). Water uptake values of C2 sample are the lowest values among all samples up to 21 days after immersion time.

## 4. Conclusions

The corrosion protection of PNC coatings containing YAG-NPs on the carbon steel was investigated in 1.0 M HCl solution by EIS technique. The YAG-NPs were synthesized by a recently developed electrochemical method. According to the protection efficiency values, the coated sample containing 0.025% YAG-NPs showed the best corrosion protection for immersion times up to 28 days.

## Acknowledgements

The authors would like to acknowledge the financial support of Iranian National Committee of Nanotechnology in Ministry of Science, Research and Technology and Islamic Azad University, Kerman Branch.

11. A.T. Ozyilmaz, M. Erbil, B. Yazıcı, The electrochemical synthesis of polyaniline on stainless steel and its corrosion performance, *Current Applied Physics*, 6(2006) 1-9.
12. A. Mohammadi, S.M.A. Hosseini, M.J. Bahrani, M. Shahidi, Corrosion inhibition of mild steel in acidic solution by apricot gum as a green inhibitor, *Prog. Color Colorants Coat.*, 9(2016) 117-134.

How to cite this article:

M. Shahidi, Gh. Golestani, A New Polymeric Nanocomposite Coating for Corrosion Protection of Carbon Steel in HCl Solution. *Prog. Color Colorants Coat.*, 11 (2018), 1-8.

